Jasim et al. Iraqi Journal of Science, 2022, Vol. 63, No. 10, pp: 4292-4304
DOI: 10.24996/ijs.2022.63.10.16

ISSN: 0067-2904

Optical and Structural Properties of Cobalt Nanoparticles Synthesized by Laser Ablation

Awatif Sabir Jasim [1], Kadhim A. Aadim [2], Sahar Naji Rashid [1*]
[1]*Department of Physics, College of Science, University of Tikrit, Tikrit, Iraq*
[2]*Department of Physics, College of Science, University of Baghdad, Baghdad, Iraq*

Received: 25/11/2021 Accepted: 19/3/2022 Published: 30/10/2022

Abstract
Pulsed laser ablation in liquid (PLAL) technique can produce high purity nanoparticles, it is a top-down physical method based on the principle of dividing metal ion bulk precursors into metal atoms, this method was used in this work to synthesis cobalt nanoparticals (CoPNs) with the use of Nd: YAG laser with two wavelengths (355 nm) and (532 nm) at energies (500 mJ) and (600 mJ) respectively, with number of pulses (1000,1100, 1200, 1300, and 1400) for each wavelength. The properties of the prepared nanoparticles were studied by UV-Vis, XRD, SEM with EDX, AFM, and FTIR analysis and then its antibacterial activity was studied by applying it on two types of bacteria with gram-positive (*Staphylococcus aureus*, *Streptococcus mutans*) and two gram-negative bacteria (*Escherichia coli*, *Pseudomonas aeruginosa*) isolated from the oral cavity. The findings showed that CoNPs prepared using the PLAL approach have antibacterial activity and could be employed to kill hazardous and pathogenic bacteria.

Keywords: Laser ablation, CoNPs, Nanotechnology, Magnetic nanoparticles, Antibacterial activity.

الخصائص البصرية والتركيبية لجسيمات الكوبالت النانوية المُصنَّعة بطريقة الاستئصال بالليزر

عواطف صابر جاسم [1], كاظم عبدالواحد عادم [2], سحر ناجي رشيد [1]*
[1]قسم الفيزياء, كلية العلوم, جامعة تكريت, تكريت, العراق
[2]قسم الفيزياء, كلية العلوم, جامعة بغداد, بغداد, العراق

الخلاصة
يمكن انتاج جسيمات نانوية عالية النقاء بتقنية الاستئصال بالليزر النبضي في السائل (PLAL) ، وهي طريقة استئصال فيزيائية من أعلى المادة (سطحها) إلى أسفل تعتمد على مبدأ تقسيم سلائف كتلة أيونات المعدن إلى ذرات معدنية ، وقد تم استخدام هذه الطريقة في هذا العمل لتخليق جزيئات الكوبالت النانوية (CoPNs) باستخدام ليزر Nd: YAG بطولين موجيين (355 نانومتر) و (532 نانومتر) وبالطاقات (500 مللي جول) و (600 مللي جول) على التوالي ، مع عدد النبضات (1000 ، 1100 ، 1200 ،

*Email: s_n_r83@yahoo.com

1300 ، و 1400 نبضة) لكل طول موجي . تمت دراسة خصائص الجسيمات النانوية المحضرة بواسطة
UV-Visو XRD وSEM و EDX و AFM و FTIR ثم دراسة نشاطها المضاد للبكتيريا عن طريق
تطبيقها على نوعين من البكتيريا ذات صبغة غرام (Staphylococcus aureus ، Streptococcus
mutans) و نوعين من البكتيريا السالبة (Escherichia coli، (Pseudomonas aeruginosa)
معزولة من تجويف الفم .أظهرت النتائج أن CoNPs المصنوعة باستخدام تقنية PLAL لها نشاط مضاد
للجراثيم ويمكن استخدامها لقتل البكتيريا الخطرة والممرضة.

1. Introduction

Nanotechnology is a multidisciplinary branch of science [1], that encompasses a wide range of scientific and technological fields [1,2]. It has become one of the most important components of scientific advancement because it employs matter manipulation on a scale where materials exhibit distinct and appealing properties when compared to others on the micro-macro scale. It has attracted a lot of attention, especially in the field of medical research [3,4], which has a huge impact on the global economy [4]. It entails the nanometer-scale modification of atomic materials to achieve the desired shape and properties for the field of application [5]. Nanoparticles (NPs) have a high specific surface area while containing a low metal mass [6], it can be used for numerous antibacterial activity applications [7,8], where it possesses a high applicability amongst cells and biomolecules [4]. Metal NPs are typically formed by reducing salts of metal found in a solution or by forming metal atom aggregates by heating or vaporizing a metal in a vacuum or an inert gas [6]. They have recently received a lot of attention due to their nontoxic nature, insensitivity to air and light, size-related electronic properties, good conductivity, chemical stability, magnetic properties, potential biological applications [9], increased surface-to-volume ratio and increased magnetic properties [10,11]. Colloidal metal NPs are of great interest to researchers from a variety of disciplines, including materials science, physics, engineering, and chemistry due to their magnetic, electronic, and optical properties [12]. One of the unique properties of metallic NPs is surface plasmon resonance (SPR) [6]. When exposed to certain light energies, free electrons collectively oscillate on the metal surface, resulting in absorption and scattering which depend on wavelength; metal NPs can highly absorb light in the region of the visible spectrum by producing collective vibration of bands of conduction in powerful resonance with fixed light frequencies [13]. The excitation of the plasmon enhances the electromagnetic field in the surrounding environment and produce measurable changes in NPs that response in the optical field [14]. Metal-based nanoparticles with potential antioxidant and antimicrobial properties have led to their incorporation into biomaterials of importance in human health care [15]. Magnetic nanoparticles have important properties that make them appealing for a wide range of antibacterial activity applications, including magnetic resonance imagining (MRI) contrast agents, cell separation and detection, and drug delivery [3]. Medical advances in nanoscience and nanotechnology rely on precise knowledge of the magnetic properties of nanoscale materials. According to research, magnetic properties at the nanoscale are fundamentally different from those at the bulk scale. As a result, the importance of nanosized biomagnetic nanoparticles (ranging from 1 to 100 nm) has drawn the attention of biotechnological researchers [1]. Among many NPs, cobalt (Co) species piqued the interest of researchers due to their diverse potential applications. Medical sensors, coatings, plastics, nanofibers, nanowires, textiles, and high-performance magnetic recording materials can all benefit from CoNPs. Because of their strong absorption of visible, infrared, and millimeter waves, cobalt oxide NPs can also be used in military applications [16]. One of CoNPs and its oxides NPs applications is in antibacterial activity [17,18]. Laser ablation is a flexible and versatile technique used to synthesis CoNPs [19], and the presence of oxygen leads to formation of the oxides of CoNPs during laser ablation [16]. The activity mechanism of antimicrobial is binding to the negatively charged bacterial cell wall, resulting in cell envelope destabilization and altered permeability [20]. Laser ablation method which can produce high purity nanoparticles without the use of a toxic chemical mixture, using a simple and low-cost synthesis process [21], which is a top-down physical method based on the principle of dividing metal ion bulk precursors into metal atoms [9,22]. Laser ablation is a promising method for producing metal colloids and NPs. It provides the critical benefit for biological applications of producing NPs with a surface that is not contaminated with reactant residue ions, as well as the processing setup costs are very low [23,24]. Laser ablation of a metal target in liquid is a novel and versatile method for preparing various nanomaterials. The most special character of this method is the non-equilibrium growth process induced by the transient plasma produced through laser ablation of a target in solution, which possesses extremely high temperature, high pressure, and high concentration of excited species [25]. The response of materials to light is affected by the power of the laser beam, as well as the temperature of the beam. Continuous laser irradiation of a material will result in a series of reactions such as heating, melting, boiling [26], and plasma formation [27]. The response of materials to a laser beam in terms of thermal effects such as melting, boiling, vaporisation, and phase-explosion of nucleation [26,28], as well as some mechanical effects such as deformation and stress in materials [26]. Figure 1 shows absorption process within matter as a function of increasing power. The thermal diffusion depth of the laser pulse (D) can be determined by the following relationship:

$$D = (4N\tau_{las})^{1/2} \quad (1)$$

Where: (D) is the thermal diffusion depth, (N) is the thermal diffusion of the material, and (τ_{las}) is the duration of the laser pulse [29].

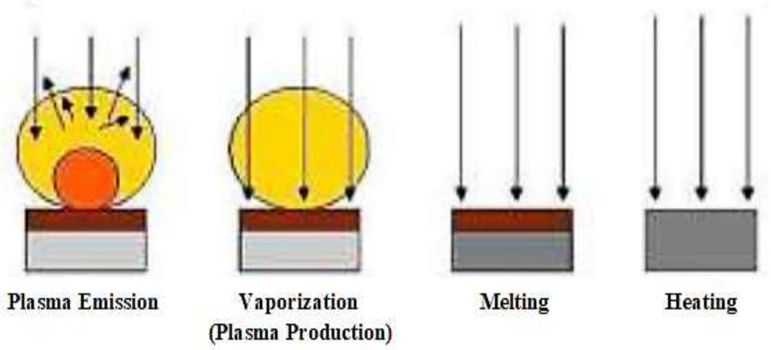

Figure 1: Absorption process within matter as a function of increasing power

The position of a metal colloidal solution's plasmon band depends on the type of liquid environment used during laser ablation. Under the same laser beam parameters, the plasmon peak of metal NPs is affected not only by the type of liquid, but also by the chemical concentration of the liquid; the plasmon band can also be changed by changing the wavelength of ablation laser light [26]. When discussing the role of solvent, it is important to remember that the high oxidization of NPs alters the effects of plasmon resonance formation. Because such oxide shells are difficult to destroy, small core-shell NPs appear to be sufficiently stable [16]. In this work, CoNPs were prepared using the laser ablation method. CoNPs physical properties and antibacterial activity were studied..

2. Materials and Methods

CoNPs were prepared using pulsed laser ablation technique in liquid (PLAL) using a pure cobalt plate with dimensions (1 cm, 1 cm, & 2 mm) placed in (5 ml) of ethanol of (99.99%)

purity in a beaker and at a distance (5 cm) from the laser source. Q-switched Nd: YAG laser was applied, rate of repetition (6 Hz), wavelengths (355, 532 nm) corresponding to energies of (500, 600 mJ), respectively and the number of pulses (1000, 1100, 1200, 1300, and 1400 Pulse) for each wavelength, as shown in Figure 2. Structural and optical analyses of the prepared samples were carried out using XRD, FESEM, EDX, AFM, UV-Vis, and FTIR techniques. CoNPs antibacterial activity on two types of gram-positive bacteria (*Staphylococcus aureus*, *Streptococcus mutans*), as well as two gram-negative bacteria (*Escherichia coli*, *Pseudomonas aeruginosa*) isolated from the oral cavity was tested.

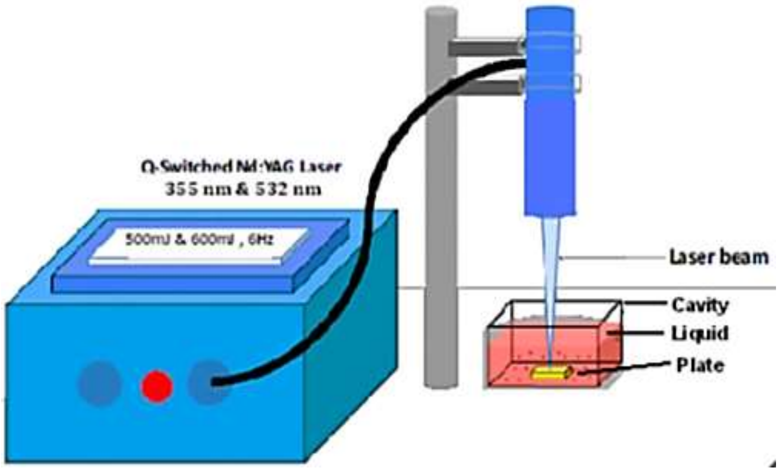

Figure 2: Schematic diagram of PLAL technique for NPs synthesized

3. Results and Discussion

3.1 UV-Vis absorption analysis

It is one of the most widely used techniques for identifying various substances, such as transition metal ions, organic compounds, and biological molecules. The first evidence of a synthesis reaction is the color change of the cobalt colloidal solutions from colorless to light yellowish brown color and then darker color by increasing the number of pulses as a result of the cobalt ablation process. Initial characterization of CoNPs and their oxides was performed by UV-Vis analysis. It was noticed, as shown in Figure 3, using Nd: YAG laser of 355 nm wavelength and energy of (500 mJ), that the maximum absorption increased with the increase of the number of pulses; its range was (277-293 nm) and the highest absorption was using (1400 pulses). While, when using the wavelength (532 nm) and energy (600 mJ) the maximum absorption ranged between (280 and 299 nm), as in Figure 4. In general, the maximum absorptions at (355 nm) were higher than those at (532 nm) which means that the sizes of NPs at this wavelength were smaller than those at (355 nm), where the maximum absorption represents the SPR of CoNPs.

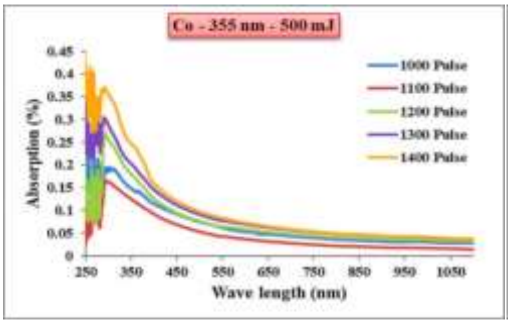

Figure 3: UV–Vis absorption spectra at 355 nm

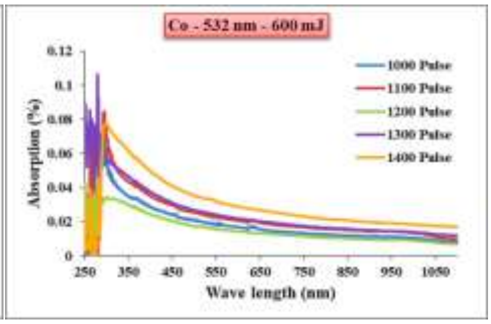

Figure 4: UV–Vis absorption spectra at 532 nm

The figures show that shorter wavelengths led to a more width uniformity of the absorption peaks with the increase of the number of pulses; the higher SPR peak with the increase of the number of pulses is attributed to a more efficient redistribution of nanoparticles due to the longer period and the accumulation of an effective electric bilayer around the NPs. This result is in agreement with that of Ali [30].

3.2 XRD analysis

Figure 5 represents the XRD patterns obtained of the synthesized CoNPs for those prepared with (355 nm – 500 mJ – 1400 Pulse) and (532 nm – 600 mJ – 1400 Pulse). A number of intensities and peaks are noted in both spectra which belong to CoNPs with a hexagonal crystal structure (the fitted XRD pattern was compared to the standard pattern, COD Card Number [96-901-2885]) and another section refers to cobalt with a triclinic (anorthic) crystal structure (COD Card Number [96-410-5681]). A number of peaks are also noted which represent cobalt oxides NPs, which are (Co_3O_4 – COD Card Number [96-900-5896]), (CoO_2 – COD Card Number [96-152-6823]), and (CoO – COD Card Number [96-152-8839]). In this figure, the apparent crystal systems, angles, and Miller's index are indicated.

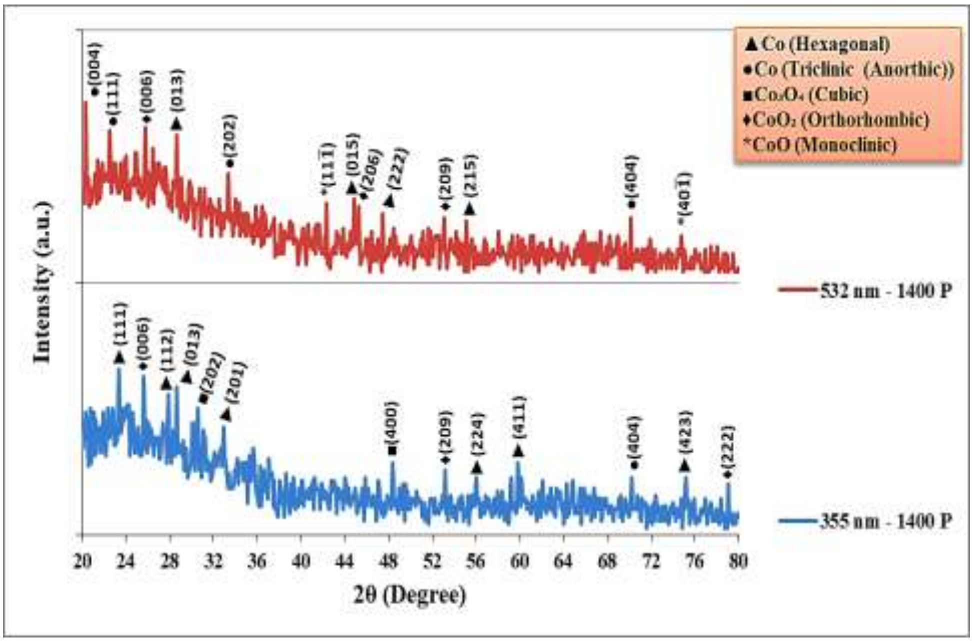

Figure 5: XRD patterns of CoNPs

The effect of laser induced oxidation is an unavoidable consequence of the laser effect on metals in the presence of air. This effect occurs as a result of the high temperatures experienced by the metal directly exposed to the laser; heat dissipation to the surroundings quickly turns in, allowing heat to propagate to the vicinity, oxidizing a metal area beyond the directly exposed and ablated channel. The results show chemical composition changes on metal surfaces as a function of net delivered fluency. The ablated material is melted and vaporized in the nanosecond regime, growing in the plasma as a result of interaction with the surrounding gas; this thermal process favors the oxidation of the ultimate NPs. This result is in agreement with that of Arias et al. [31]. Korkmaz and Karadag [10] stated that the formation of metal oxides NPs was caused by the interaction of metal atoms with oxygen atoms or radicals during their decomposition in liquid. They also stated that the type of oxide formed depends on the temperature and oxygen partial pressure.

3.3 SEM analysis

SEM images of the synthesized CoNPs were obtained to determine its morphology. Figures 6,7 show that the synthesized particles, which were ablated in ethanol, to be nanospheres, and the particle size variation is widely distributed. Also the particle size distribution indicates that the NPs average size was (28.5 nm) at (355 nm), and (52.7 nm) at (532 nm).

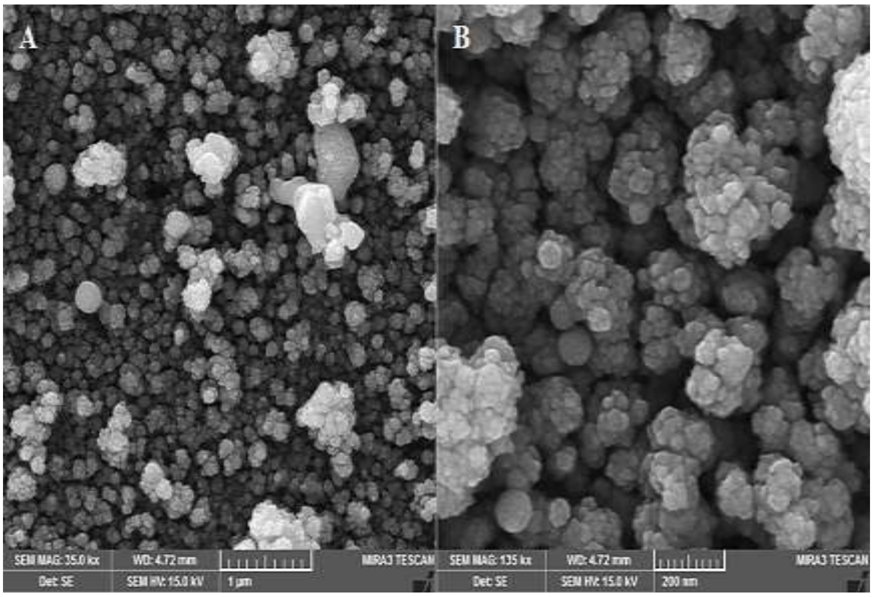

Figure 6: SEM images of CoNPs at 355 nm-500 mJ-1400 P zoom (A)1µm (B)200nm

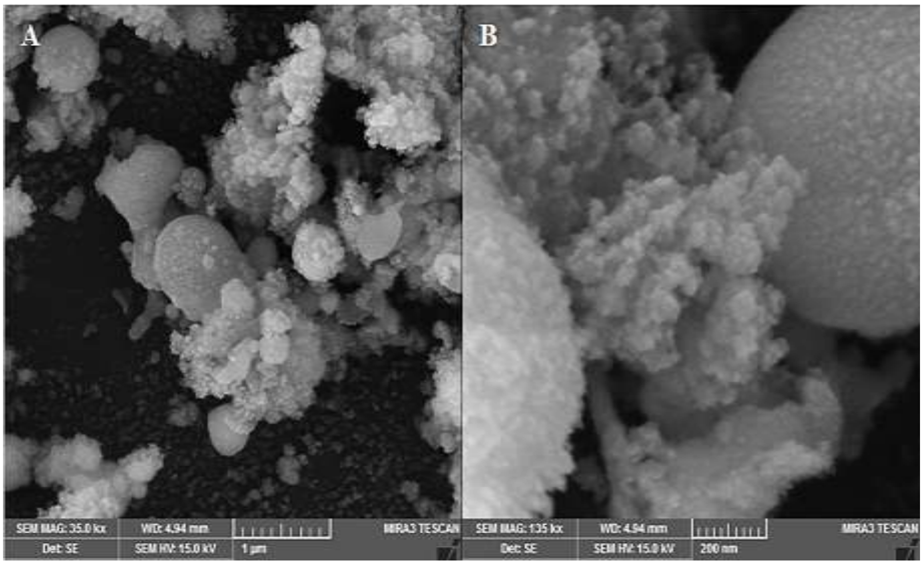

Figure 7: SEM images of CoNPs at 532 nm-600 mJ-1400 P zoom (A)1µm (B)200nm

From the above two figures, it was found that the prepared particles using the highest number of pulses led to the production of NPs of small sizes and structures, which later helps in the speed and ease of absorption and interaction with the bacterial cell wall, also noted that the shorter wavelength led to smaller and more regular nanoscale sizes and structures.

The EDX analysis determined the elemental compositions of CoNPs as shown in Figures (8 and 9), the long peak indicates the presence of cobalt in the prepared sample, it shows in general, that the apparent concentrations of the samples prepared at (355 nm) are clear.

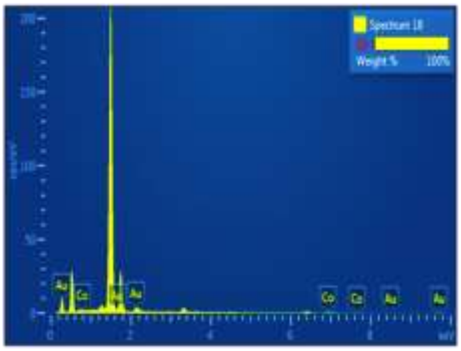
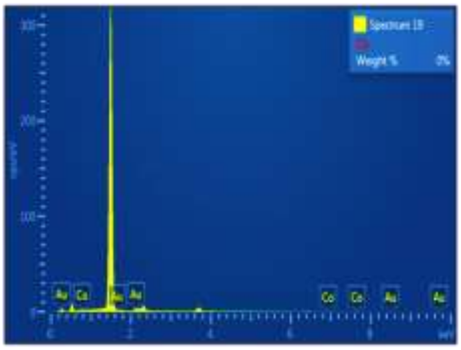

Figure 8: EDX analysis at 355nm-1400P **Figure 9** :EDX analysis at 532nm-1400P

3.4 AFM analysis

From Figures 10 and 11, it was noticed that the samples prepared at higher number of pulses are much more uniform and dense. It can be said that the surface topography analysis showed that the surface grain size was higher at the shorter wavelength, where the grain size of the prepared CoNPs at (355 nm – 500 mJ) was (72.22 nm) using (1400 pulses); while, it was (67.27 nm) at (532 nm – 600 mJ) using (1400 pulses).

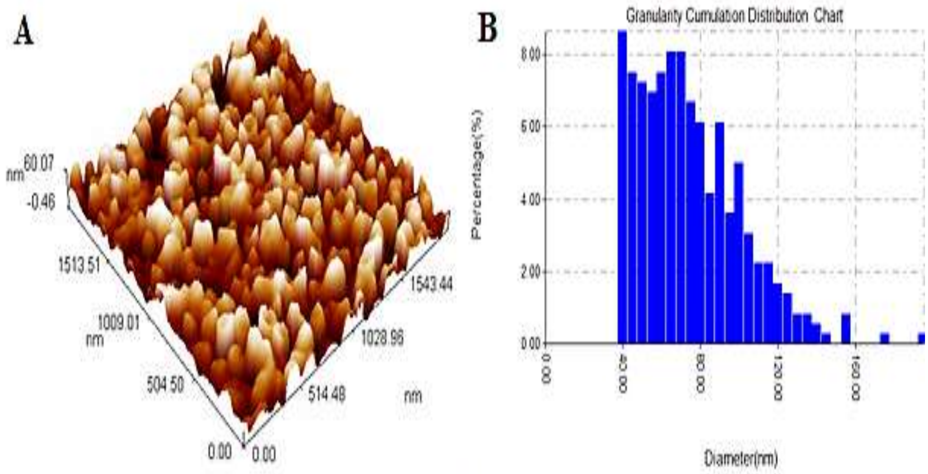

Figure 10: AFM analysis at 355 nm-500 mJ-1400 P (A) 3D image, (B) Granularity cumulative distribution

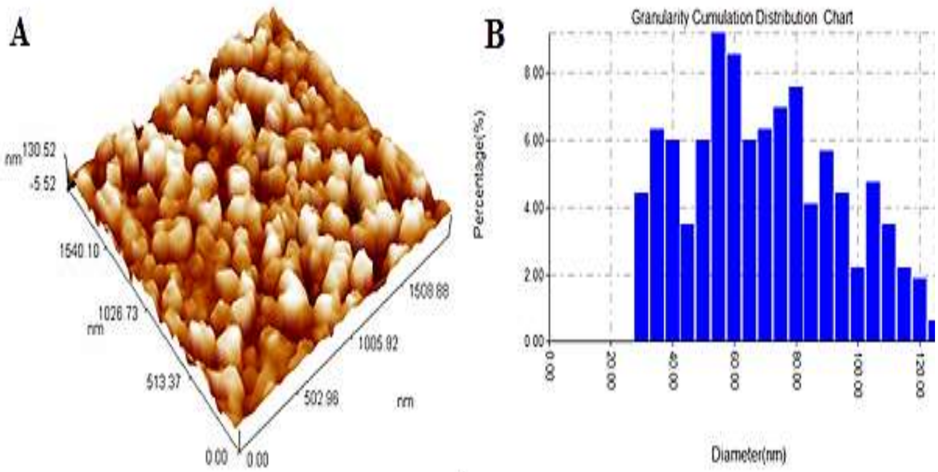

Figure 11: AFM analysis at 532 nm-600 mJ-1400 P (A) 3D image, (B) Granularity cumulative distribution

3.5 FTIR analysis

Figures 12 and 13 represent FTIR analysis of CoNPs obtained at (355 nm – 500 mJ) and (532 nm – 600 mJ), respectively, where this analysis is used for the characterizing of the surface chemistry of nanoparticles.

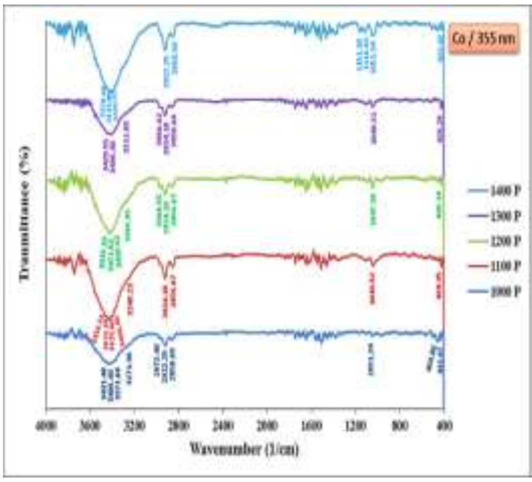

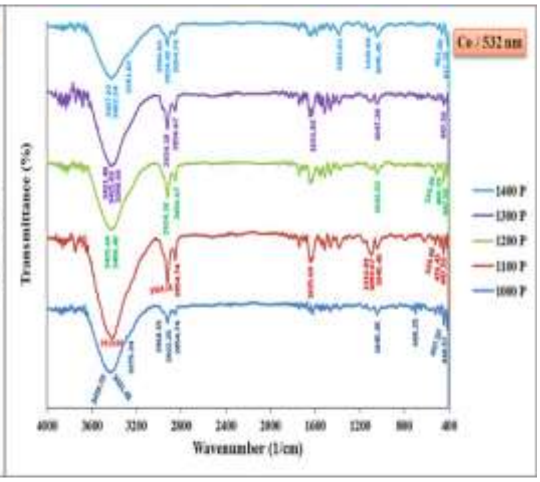

Figure 12: FTIR analysis at 355 nm-500 mJ **Figure 13:** FTIR analysis at 532 nm-600 mJ

FTIR spectra in both figures showed absorption peaks corresponding to the group of hydroxyl (O-H), alkane (C-H), and aliphatic amines (C-O) stretching vibrations, in addition to carboxylic acid (C=O) stretching group in Figure 13 in the synthesis of NPs process. Also, in both figures, the band below (600 cm^{-1}) is due to the formation of CoNPs and its oxides. The number of pulses affects the value of the absorption peaks, the appearance, disappearance of some of them, and the concentration of solutions.

3.6 Energy gap (Eg)

As it was noticed from the analysis of XRD, beside CoNPs, cobalt oxides NPs were also formed in the samples prepared in this work, and to calculate the energy gap (Eg) for these oxides, absorption as a function of wavelength was plotted, as in Figures 14 and 15 using the following equation [32]:

$$Eg\ (eV) = 1240 / \lambda_g\ (nm) \tag{2}$$

Where: λ_g is the absorption edge calculated as the intersection of the absorption curve's tangent and the abscissa coordinate [33]. In general, we found that Eg at (355 nm – 500 mJ) was in the range (2.48 – 3.88 eV), and these values were fluctuating with increasing the number of pulses. But at (532 nm – 600 mJ) the range was (1.88 – 2.95 eV), where the values here decreased regularly by increasing the number of pulses. So, the results showed that a higher Eg of cobalt oxides NPs at (355 nm) can be obtained under the conditions of this work.

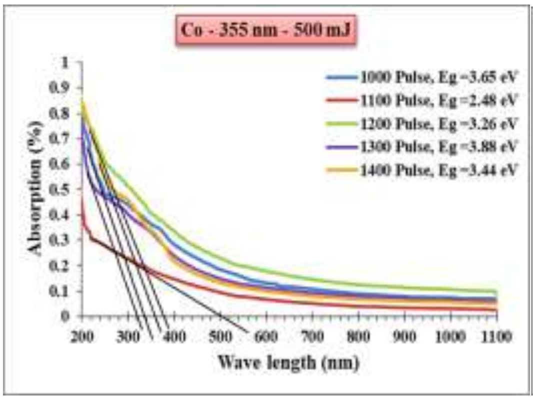

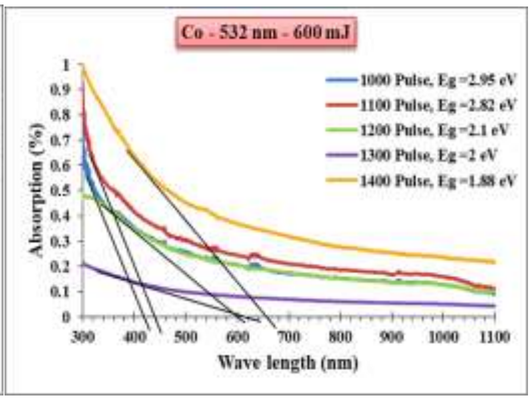

Figure 14: Energy gap of Co oxides NPs at 355 nm

Figure 15: Energy gap of Co oxides NPs at 532 nm

3.7 Antibacterial activity

The results of the antibacterial activity showed that the prepared CoNPs prepared did not have significant inhibiting activity on the four mentioned bacteria (*S. aureus*, *S. mutans*, *E. coli*, *and Pseudomonas*); this may be due to increased bacterial resistance proven by antibiotic sensitivity test (not found in this research). However, the inhibition zones of CoNPs prepared by laser ablation for both wavelengths and for all mentioned number of pulse can be observed, as shown in Figures 16 and 17.

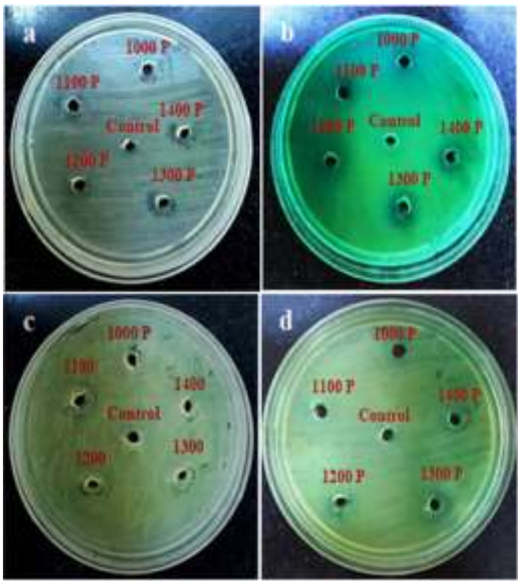

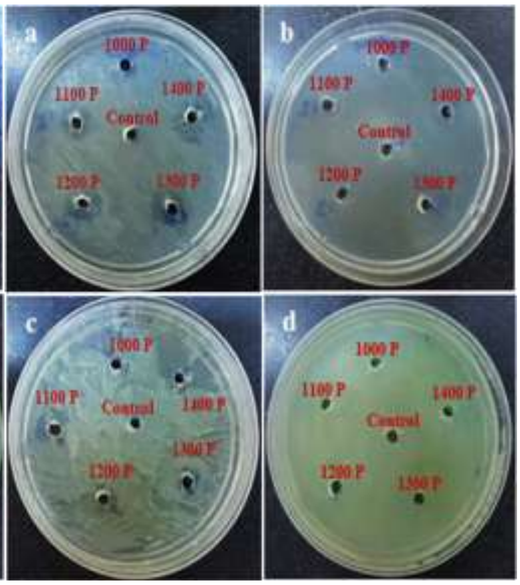

Figure 16: Antibacterial activity at 355 nm-500 mJ
(a)*S. aureus* (b)*S. mutans* (c)*E. coli* (d)*Pseudomonas*

Figure 17: Antibacterial activity at 532 nm-600 mJ
(a)*S. aureus* (b)*S. mutans* (c)*E. coli* (d)*Pseudomonas*

From these two figures, we note that CoNps affected bacteria in different proportions, and the nanoparticles prepared at the wavelength (355 nm) were more effective as they affected all species because of the smaller particle size ratio, while at the wavelength (532 nm), it was found that (*Pseudomonas*) bacteria were not affected by the prepared nanoparticles as they did not show inhibition zones; also, (*S. mutans*) was only affected with using (1100 pulses). The diameters of the bacteria lining areas were calculated as in Figures 18 and 19. An increase in the diameters of the inhibition zones indicating an increase in antibacterial activity was noticed as the number of pulses was increased that resulted in the increase in the concentration of NPs.

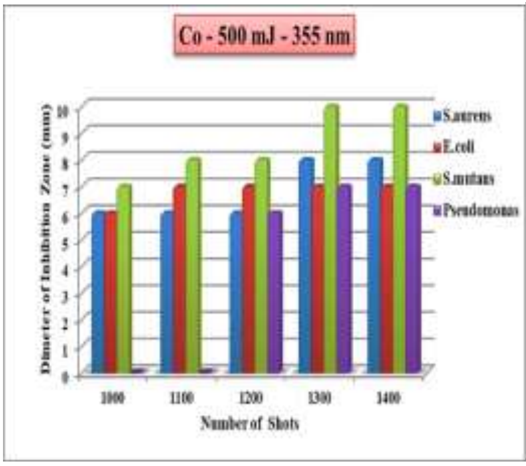

Figure 18: Antibacterial activity histogram at 355nm

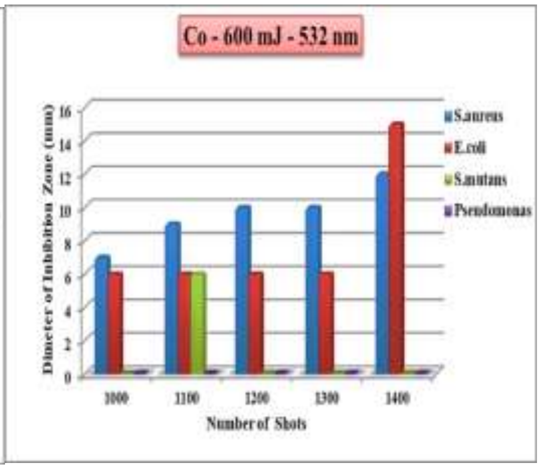

Figure 19: Antibacterial activity histogram at 532nm

4. Conclusions

This work synthesized CoNPs by the physical method that is PLAL, and its antibacterial activity was studied. The results showed the possibility of obtaining CoNPs using two wavelengths of Nd: YAG laser (355 nm and 532 nm) in the process of ablation and with different numbers of pulses through the change of the color of the solution as a preliminary proof of the nanosynthesis of the material. This laser treatment led to the formation of cobalt nano oxides as well, and whose energy gaps were calculated. FTIR analysis was conducted and it was found that the effective groups present in the prepared samples were (O-H, C-H, C-O, and C=O). As for the structural analysis that were conducted, they included XRD, SEM with EDX, and AFM for selected samples, which were prepared with the highest number of pulses. The nanoparticles prepared using the highest number of pulses gave the highest antibacterial activity for both wavelengths used. In general, it can be said that the prepared samples at wavelength (355 nm) are the most effective under the conditions of this work. The results obtained proved that pulsed laser ablation is an easy and fast method for metal nanosynthesis and it can be a good alternative to other methods, and the NPs prepared with it have antibacterial activity efficacy, however, additional studies may be needed to change the laser parameters and study other applications.

5. Acknowledgements

The authors thank those in charge of the laboratories of the Departments of Physics and Biology at the College of Science – University of Tikrit; for facilitating the use of what was required to complete this work.

6. Disclosure and conflict of interest

“Conflict of Interest: The authors declare that they have no conflicts of interest.”

References

[1] A. Nochehdehi, S. Thomas, M. Sadri, S. Afghahi and S. Mehdi, "Iron Oxide Biomagnetic Nanoparticles (IO-BMNPs); Synthesis, Characterization and Biomedical Application–A Review," *J Nanomed Nanotechnol*, vol. 8, no.1, pp. 1-9, 2017, DOI:10.4172/2157-7439.1000423.

[2] S. Agrawal, M. Bhatt, S. Rai, A. Bhatt, P. Dangwal and P. Agrawal, "Silver nanoparticles and its potential applications: A review," *J. of Pharmacognosy and Phytochemistry*, vol. 7, no. 2, pp. 930-937, 2018, https://www.phytojournal.com/archives?year=2018&vol=7 &issue=2&ArticleId =3470.

[3] L. S. Arias, J. P. Pessan, A. P. M. Vieira, T. M. T. de Lima , A. C. B. Delbem and D. R. Monteiro, "Iron Oxide Nanoparticles for Biomedical Applications: A Perspective on Synthesis, Drugs, Antimicrobial Activity, and Toxicity," *Antibiotics (MDPI)*, vol. 7, no. 46, pp. 1-32, 2018, doi:10.3390/antibiotics7020046.

[4] L. S. Ganapathe, M. A. Mohamed, R. M. Yunus and D. D. Berhanuddin, "Magnetite (Fe3O4) Nanoparticles in Biomedical Application: From Synthesis to Surface Functionalisation," *Magnetochemistry*, vol. 6, no. 68, pp. 1-35, 2020, doi:10.3390/magnetochemistry6040068.

[5] K. McNamara and S. A. M. Tofail, "Nanoparticles in biomedical applications," *Advances in Physics: X*, vol. 2, no. 1, pp. 45-88, 2016, doi.org/10.1080/23746149.2016.1254570.

[6] S. Nakamura, M. Sato, Y. Sato, N. Ando, T. Takayama, M. Fujita and M. Ishihara, "Synthesis and Application of Silver Nanoparticles (Ag NPs) for the Prevention of Infection in HealthcareWorkers," *Int. J. Mol. Sci.*, vol. 20, 3620, 2019, doi:10.3390/ijms20153620.

[7] Laurent, Bridot, V. Elst and Muller, "Magnetic iron oxide nanoparticles for biomedical applications," *Future Med. Chem.*, vol. 2, no. 3, pp. 427-449, 2010, doi:10.4155/fmc.09.164.

[8] G. Bagherzade, M. M. Tavakoli and M. H. Namaei, "Green synthesis of silver nanoparticles using aqueous extract of saffron (*Crocus sativus* L.) wastages and its antibacterial activity against six bacteria," *Asian Pacific Journal of Tropical Biomedicine*, vol. 7, no. 3, pp. 227-233, 2017, doi.org/10.1016/j.apjtb.2016.12.014.

[9] W. Norsyuhada W. M. Shukri, H. Bakhtiar, S. Islam and N. Bidin, "Synthesis and Characterization of Gold-Silver Nanoparticles in Deionized Water by Pulsed Laser Ablation (PLAL) Technique at Different Laser Parameter," *International Journal of Nanoscience*, vol. 17, no. 3, pp. 1850015 (9 pages), 2018, DOI:10.1142/S0219581X18500151.

[10] N. Korkmaz and A. Karadag, "Microwave Assisted Green Synthesis of Ag, Ag_2O, and Ag_2O_3 Nanoparticles," *Journal of the Turkish Chemical Society*, vol. 8, no. 2, pp. 585-592, 2021, doi.org/10.18596/jotcsa.784065.

[11] Atul, M. Kumar and A. Sharma, "Indresh Kumar Maurya, Alpana Thakur and Sunil Kumar, Synthesis of ultra small iron oxide and doped iron oxide nanostructures and their antimicrobial activities," *Journal of Taibah University for Science*, 13, no. 1, pp. 280-285, 2019, DOI:10.1080/16583655.2019.1565437.

[12] M. Vinod and K.G. Gopchandran, "Au, Ag and Au:Ag colloidal nanoparticles synthesized by pulsed laser ablation as SERS substrates," *Progress in Natural Science: Materials International*, vol. 24, pp 569-578, 2014, doi.org/10.1016/j.pnsc.2014.10.003.

[13] A. Al-Sharqi, K. Apun, M. Vincent, D. Kanakaraju and L. M. Bilung, "Enhancement of the Antibacterial Efficiency of Silver Nanoparticles against Gram-Positive and Gram-Negative Bacteria Using Blue Laser Light," *International Journal of Photoenergy*, Vol. 2019, Article ID 2528490, 12 pages, doi.org/10.1155/2019/2528490.

[14] D. O. Samson, T. O. Adeeko and E. K. Makama, "Synthesis and Optical Characterization of Silver Nanoparticles (Ag-NPs) Thin Films (TFs) Prepared by Silar Technique," *International Journal of Current Research and Academic Review*, vol. 5, no. 12), pp. 15-24, 2017, doi.org/10.20546/ijcrar.2017.512.003.

[15] P. K. Dara, R. Mahadevan, P. A. Digita, S. Visnuvinayagam, L. R. G. Kumar, S. Mathew, C. N. Ravishankar and R. Anandan, "Synthesis and biochemical characterization of silver nanoparticles grafted chitosan (Chi-Ag-NPs): in vitro studies on antioxidant and antibacterial applications," *SN Applied Sciences*, vol. 2, no. 665, 12 pages, 2020 doi.org/10.1007/s42452-020-2261-y.

[16] K. Rao, R. Ganeev, K. Zhang, Y. Fu, G. Boltaev, P. Krishnendu, P. Redkin and C. Guo, "Laser ablation–induced synthesis and nonlinear optical characterization of titanium and cobalt nanoparticles," *J Nanopart Res*, vol. 20, no. 285, pp. 1-15, 2018, doi.org/10.1007/s11051-018-4391-3.

[17] M. Raza, Z. Kanwal, S. Riaz and S. Naseem, "Synthesis, characterization and antibacterial properties of nano-sized cobalt particles," *Advances in civil, environmental and material research (ACEM16)*, vol. 1, 7 pages, 2016, https://www.researchgate.net/publication/308198435_Synthesis_characterization_and_antibacterial_properties_of_nano-sized_cobalt_particles.

[18] S.M. Ansari, R.D. Bhor, K.R. Pai, D. Sen, S. Mazumder, K. Ghosh, Y.D. Kolekar and C.V. Raman, "Cobalt nanoparticles for biomedical applications: Facile synthesis, physiochemical characterization, cytotoxicity behavior and biocompatibility," *Applied Surface Science*, vol. 414, pp. 171-187, 2017, doi.org/10.1016/j.apsusc.2017.03.002.

[19] H. Zhang, C. Liang, J. Liu, Z. Tian and G. Shao, "The formation of onion-like carbon-encapsulated cobalt carbide core/shell nanoparticles by the laser ablation of metallic cobalt in acetone," *Carbon*, vol. 55, pp. 108-115, 2013, doi.org/10.1016/j.carbon.2012.12.015.

[20] R. Kalaivani, M. Maruthupandy, T. Muneeswaran, A. H. Beevi, M. Anand, C.M. Ramakritinan, A. K. Kumaraguru, "Synthesis of chitosan mediated silver nanoparticles (Ag NPs) for potential antimicrobial applications," *Frontiers in Laboratory Medicine*, vol. 2, pp. 30-35, 2018, doi.org/10.1016/j.flm.2018.04.002.

[21] M. Z. Alhamid, B. S. Hadi, and A. Khumaeni, "Synthesis of silver nanoparticles using laser ablation method utilizing Nd:YAG laser," *AIP Conference Proceedings*, vol. 2202, 020013, 2019, doi.org/10.1063/1.5141626.

[22] A. M. Brito-Silva, L. A. Gomez, C. B. de Araujo and A. Galembeck, "Laser Ablated Silver Nanoparticles with Nearly the Same Size in Different Carrier Media," *J. of Nanomaterials*, 7 pages, 2010, doi:10.1155/2010/142897.

[23] F. H. Abd El-kader, N.A. Hakeem, I. S. Elashmawi and A. A. Menazea, "Synthesis and characterization of PVK/AgNPs nanocomposites prepared by laser ablation," *Spectrochimica Acta Part A: Molecular and Biomolecular Spectroscopy*, vol. 138, pp. 331-339, 2015, doi.org/10.1016/j.saa.2014.11.083.

[24] A. Al-Kattan, G. Tselikov, K. Metwally, A. A. Popov, S. Mensah and A. V. Kabashin, "Laser Ablation-Assisted Synthesis of Plasmonic Si@Au Core-Satellite Nanocomposites for Biomedical Applications," *Nanomaterials*, vol. 11, no. 592, pp. 1-12, 2021, doi.org/10.3390/nano11030592.

[25] H. Zeng, S. Yang and W. Cai, "Reshaping Formation and Luminescence Evolution of ZnO Quantum Dots by Laser-Induced Fragmentation in Liquid," *J. Phys. Chem.*, vol. 115, pp. 5038-5043, 2011, doi.org/10.1021/jp109010c.

[26] A. H. Hamad, "Picosecond Laser Generation and Modification of Ag-TiO2 Nanoparticles for Antibacterial Application," *PhD thesis, School of Mechanical, Aerospace and Civil Engineering, The University of Manchester*, 2017, https://www.escholar.manchester.ac.uk/uk-ac-man-scw:307073.

[27] K. A. Aadim, "Characterization of Laser induced cadmium plasma in air", *Iraqi Journal of Science*, vol. 56, no. 3, pp. 2292-2296, 2015, https://www.iasj.net/iasj/download/1d408c8373f54406.

[28] E. M. Mahdi, S. N. Rashid, A. S. Jasim, "Effect Of Nd:YAG Laser On Ants (*Camponotus consobrinus*)", *Iraqi Journal of Science*, vol. 62, no. 11(Special Issue), pp. 4313-4322, 2021, DOI.10.24996/ijs.2021.62.11(SI).12.

[29] A. S. Jasim, S. N. Rashid and A. J. Asaad, "Study the Interaction of CO2 Laser with ZnO Thin Films and Its Effect on Its Topographic and Optical Properties," *Proceeding of First International and the Third Scientific Conference, College of Science - University of Tikrit*, pp. 139-146, 2018, https://www.researchgate.net/publication/342902881_Study_the_Interaction_of_CO_2_Laser_with_ZnO_Thin_Films_and_Its_Effect_on_Its_Topographic_and_Optical_Properties.

[30] A. K. Ali, "Preparation of Ag and Au Nanoparticles by Pulsed Laser Ablation in Liquids," *PhD theses, Department of Applied Sciences at the University of Technology*, 2010, doi.10.13140/RG.2.2.22939.52004.

[31] M. Arias, M. Boutinguiza, J. del Val, A. Riveiro, D. Rodríguez, F. A.González , J. Gil and J. Pou, "Fabrication and Deposition of Copper and Copper Oxide Nanoparticles by Laser Ablation in Open Air," *Nanomaterials (MDPI)*, vol. 10, no. 300, pp. 1-16, 2020, doi:10.3390/nano10020300.

[32] Z. Zhang, H. Liu, X. Wang, J. Zhang, M. Yu, S. Ramakrishna and Y. Long, "One-Step Low Temperature Hydrothermal Synthesis of Flexible TiO2/PVDF@MoS2 Core-Shell Heterostructured Fibers for Visible-Light-Driven Photocatalysis and Self-Cleaning," *Nanomaterials*, vol. 9, no. 431, 22 pages, 2019, doi:10.3390/nano9030431.

[33] S. B. Dangi, K. K. Khichar, U. Kumar, S. Z. Hashmi, B. L. Choudhary, S. Kumar and P. A. Alvi, "Investigation of optical properties of PVA-GO nanocomposites," *AIP Conference Proceedings*, vol. 2220, 020082 (6 pages), 2020, doi.org/10.1063/5.0001129.